



## Environmental radioactivity, magnetic measurements and mineral analysis of major South Indian river sediments

S. Murugesan<sup>1,\*</sup>, S. Mullainathan<sup>2</sup>, V. Ramasamy<sup>3</sup> and V. Meenakshisundaram<sup>4</sup>

<sup>1</sup>Department of Physics, Sathiyabama University, Chennai – 600 119, Tamilnadu, India

<sup>2</sup>Department of Physics, A.V.C.College of Engineering, Mayiladuthurai-609305, Tamilnadu, India

<sup>3</sup>Department of Physics, Annamalai University, Annamalainagar – 608002, Tamilnadu, India

<sup>4</sup>Health and Safety Division, Indira Gandhi Centre for Atomic Research, Kalpakkam – 603102, Tamilnadu, India

Received 23 Dec 2014, Revised 09 Apr 2016, Accepted 02 May 2016

\*Corresponding author. E-mail: [binunair.phd@gmail.com](mailto:binunair.phd@gmail.com)

### Abstract

The activity concentrations of <sup>238</sup>U, <sup>232</sup>Th and <sup>40</sup>K have been determined by Gamma ray spectrometer with NaI (Tl) detector in sediments of Palar river, Tamilnadu, India. The mean values of <sup>238</sup>U, <sup>232</sup>Th and <sup>40</sup>K are 9.81±0.3, 36.49±2.4 and 742.46±26.5 Bqkg<sup>-1</sup>. The absorbed dose rate, radium equivalent concentration, external (H<sub>ex</sub>) and internal (H<sub>in</sub>) hazardous indices are calculated and compared with the world average. The radioactive heat production rate (RHP) and Excess Lifetime Cancer Risk (ELCR) are also calculated. The observed dose rate from ERDM (Environmental Radiation Dosi Meter) at 1m above the ground level are measured and correlated with calculated absorbed dose rate. The distribution of quartz, feldspar, magnetic susceptibility and weight of the magnetic minerals are correlated with radioactivity results. From the observations, the weight of the magnetic minerals is an index to select the sediments of low or high radiological risk. The mean activity concentrations and the values obtained from the criteria formula is slightly greater than the world average.

**Keywords:** Sediments; Palar River; Radioactive heat production rate (RHP); Excess Lifetime Cancer Risk (ELCR); Quartz; Magnetic susceptibility;

### 1. Introduction

Radiation of natural origin at the earth's surface consists of two components namely cosmic rays and radiation from the radioactive nuclides in the earth's crust. The later component, terrestrial radiation, mainly originates from primordial radioactive nuclides that were made in the early stage of the formation of solar system. Uranium, thorium and potassium are, however, the main elements contributing to natural terrestrial radioactivity[1]. Studies of terrestrial natural radiation are of great importance for several reasons[2].

Animals and human receive natural background radiation doses from cosmic rays, gamma rays arising from rocks and soil, inhalation of radon gas, ingestion of radionuclides with food, water, and soil. Animals often receive higher doses than human because they ingest more soil or sediment with food items, which raises their body burden of radionuclides. In addition, they live in outdoors, which increases their exposure to cosmic rays and terrestrial gamma radiation. The radiological implication of the above nuclides is due to radiation exposure of the body by gamma rays and irradiation of lung tissue from inhalation of radon and its daughters. Therefore, the assessment of gamma radiation doses from natural sources is of particular importance as natural radiation is the largest contributor to the external dose of the world population [3].

Measurements of activity concentration due to gamma rays from these materials and consequently the determination of dose rate are needed to implement precautionary measures whenever the dose is found to be above the world average. The present investigation is focused on river sediments and it is a main material in all types of constructions in India. Thus, the aim of this study is to determine the activity concentrations, absorbed and observed dose rates, radium equivalent activities (Ra<sub>eq</sub>), hazard indices and RHP rate and Excess Lifetime Cancer Risk (ELCR) in Palar river sediments of Tamilnadu, India. An attempt has also been made to find out the relation of magnetic susceptibility and weight of the magnetic particles with activity concentration measurements, absorbed dose rate and distribution of quartz and feldspar.

## 2. Materials and methods

Fig. 1 shows the geographic location of the sampling sites. Each site is separated by a distance of 20 kms approximately. At each site, a sampling area of 1m<sup>2</sup> was considered from upper and lower (2 feet depth) of right, center and left of the rivers and totally 6 wet samples were taken for analysis. Each sample has about 2 kg. Then the sample was dried in an oven at 100-110°C for about 24 hours and sieved through a 2-mm mesh to remove stone, pebbles and other macro-impurities. The homogenized sample was placed in a 250ml airtight PVC container. The inner lid was placed in and closed tightly with outer cap. The container was sealed hermitically and externally using cellophane tape and kept aside for about a month to ensure equilibrium between Ra and its daughter products before being taken for gamma ray spectrometric analysis.

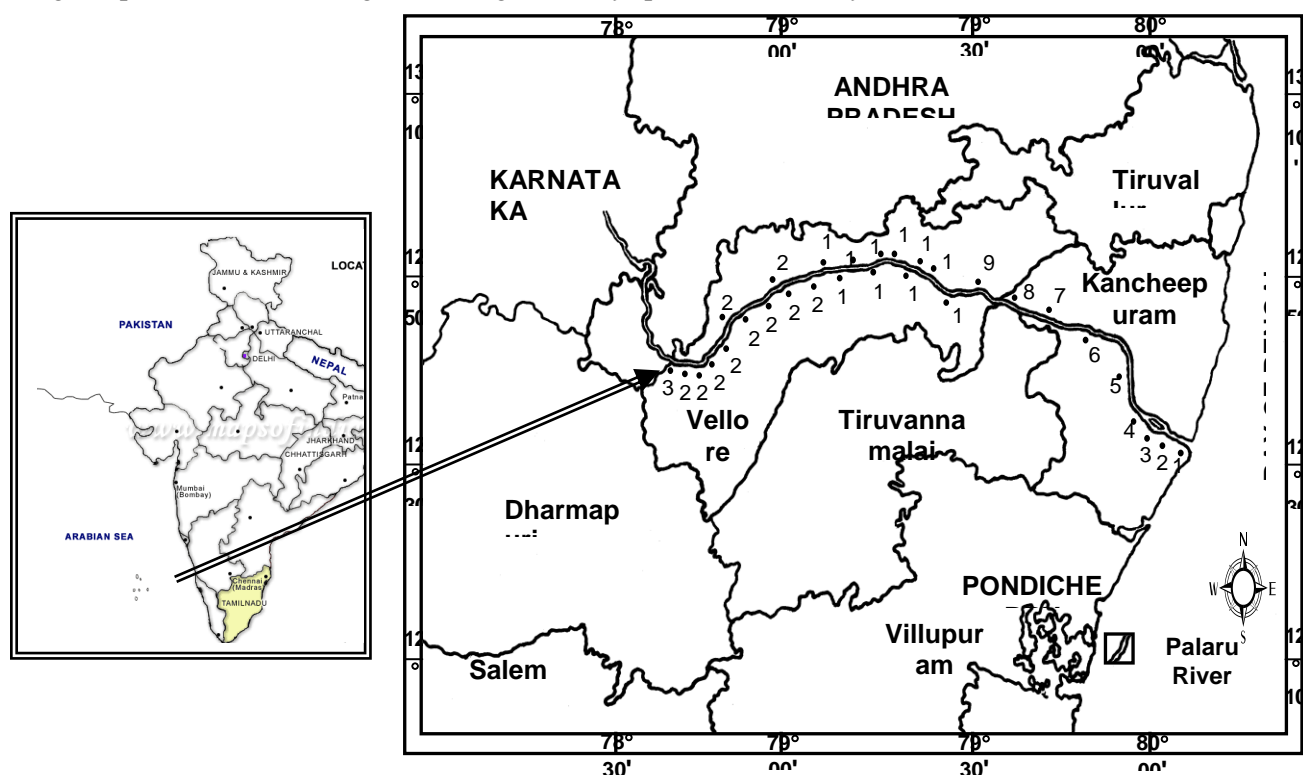


**Figure 1.** Location of Palar river in Tamilnadu, India

The activity concentrations of primordial radio nuclides (<sup>238</sup>U, <sup>232</sup>Th and <sup>40</sup>K) in the samples were determined by employing NaI (TI) gamma ray spectrometer system coupled to a 4K multi channel analyzer (ORTEC MODEL 7 450) . The detector was housed inside a massive lead shield to reduce the background of the system. It was calibrated using a standard solution of <sup>226</sup>Ra in equilibrium with its daughters. At each sampling site the ambient gamma radiation level was measured using a digital environmental radiation dosimeter (ERDM). The ERDM is calibrated regularly before starting the survey using standard sources <sup>137</sup>Cs and <sup>60</sup>Co. The ERDM readings are recorded at 1m above ground level. Five readings are taken at each site and the average was recorded.

To record the IR spectra, the samples were ground in acetone to a particle size of 53µm with small agate balls in an agate vial and kept at 4 °C to prevent heating and structural changes. The KBr pressed disc technique is used. The powder is then mixed with KBr in agate mortar with 1:20 ratio. Using Nicolate Avatar – 360 series FTIR spectrophotometer, the IR spectra of all the samples are recorded in the region 4000-400 cm<sup>-1</sup>. The resolution of the instrument is 2 cm<sup>-1</sup>.

Magnetic susceptibility measurements were carried out using a magnetic susceptibility meter MS2, Bartington Instruments Ltd., linked to MS2B dual frequency sensor (470 and 4 700 Hz). The dried river sediments sampled with paleomagnetic plastic boxes (8cm<sup>3</sup>) was placed in a magnetic field of 100 mT, which is produced by partial ARM device attached to a shielded demagnetiser, Molspin Ltd. The weight of the magnetic minerals was separated from 20g using electromagnet to demonstrate its relationship with magnetic susceptibility and radioactivity.

### 3. Results and discussion

#### 3.1 Activity concentration of primordial radionuclides

The activity concentration of the radio nuclides  $^{238}\text{U}$ ,  $^{232}\text{Th}$  and  $^{40}\text{K}$  in  $\text{Bqkg}^{-1}$ , corresponding absorbed dose rates in  $\text{nGyh}^{-1}$  and annual effective equivalent dose in  $\mu\text{Svy}^{-1}$  are tabulated in Table 1. As listed in the Table 1, the activity concentrations are ranged from  $5.64 \pm 0.4$  to  $18.44 \pm 0.4 \text{ Bqkg}^{-1}$  with a mean value of  $9.81 \pm 0.3 \text{ Bqkg}^{-1}$ ,  $6.13 \pm 1.2$  to  $254.06 \pm 5.6 \text{ Bqkg}^{-1}$  with a mean value of  $36.49 \pm 2.4 \text{ Bqkg}^{-1}$  and  $483.49 \pm 24.3$  to  $884.78 \pm 28.2 \text{ Bqkg}^{-1}$  with a mean value of  $742.46 \pm 26.5 \text{ Bqkg}^{-1}$  for  $^{238}\text{U}$ ,  $^{232}\text{Th}$  and  $^{40}\text{K}$  respectively and are shown in Fig. 2. In the present study except site no.7 the activity concentrations are almost lower than the countries like China, Greece, France and Bangladesh and those values are given Table 3. [2-10].

The mean activity concentration of  $^{238}\text{U}$  is 0.28 times lower than the world average (UNSCEAR, 2000)<sup>1</sup> and 0.66 times lower than the all India average value [11] whereas the mean of  $^{232}\text{Th}$  is 1.22 times and 1.99 times higher. The mean concentration of  $^{40}\text{K}$  is 1.85 times higher than the world average. This shows that the  $^{40}\text{K}$  dominates over  $^{238}\text{U}$  and  $^{232}\text{Th}$  like what normally happens in soil.

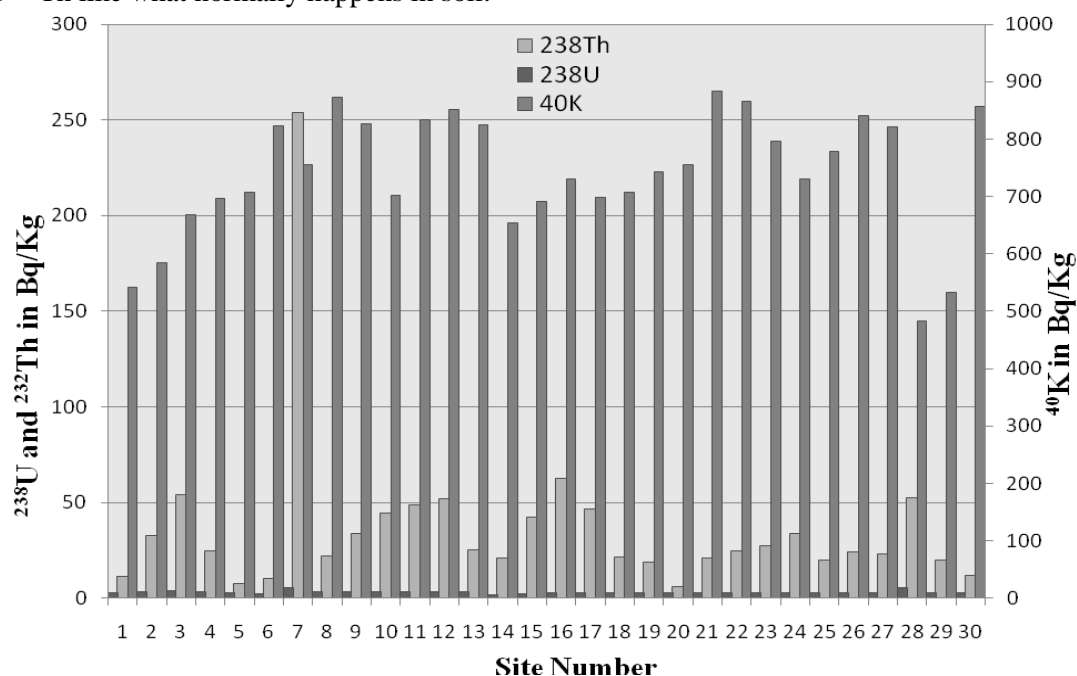


Figure 2. Graph of activity concentration for different locations

#### 3.2 Correlation between activity concentrations

The correlation between  $^{238}\text{U}$  and  $^{232}\text{Th}$  is found to be weak ( $R^2 = 0.426$ ) which indicates minimum contribution of monazite mineral in the sample (Fig.3). The values are almost less than unity, because  $^{232}\text{Th}$  activities are usually greater than  $^{238}\text{U}$  activities in the crust, which is the origin of the river. This implies that relative mobility of uranium (largely dissolved) and thorium (largely particulated) depends upon prevailing hydrological region. The adsorption of uranium by clay minerals, insoluble oxides, oxihydroxides and organic matters may be due to leaching of sediments from weathering, erosion and transport in the surfacial environments. Uranium is quite soluble in oxidizing natural waters, whereas thorium is much less soluble.

The  $^{40}\text{K}/^{232}\text{Th}$  ratio has a special significance and varies linearly with clay minerals. Because, the concentration of  $^{40}\text{K}$  and  $^{232}\text{Th}$  is depends upon the relative amounts of the feldspars, mica and clay minerals. During the weathering process,  $^{40}\text{K}$  is more soluble and is easily carried away in water, whereas  $^{232}\text{Th}$  tends to remain.  $^{40}\text{K}/^{232}\text{Th}$  is changing considerably from feldspar (low) to kaolinite (high). In the present study, higher value (site nos. 5, 6 and 20) of  $^{40}\text{K}/^{232}\text{Th}$  may indicate the presence of feldspars or clay or combination of both as maximum. These results are confirmed by FTIR analysis. The activity ratio of  $^{40}\text{K}/^{238}\text{U}$  and  $^{40}\text{K}/^{232}\text{Th}$  give no obvious trend with poor correlation [12].

**Table 1:** The Activity concentration, calculated absorbed dose rates, observed dose rates and the annual effective equivalent dose

S.No.	Location	Latitude	Longitude	U BqKg <sup>-1</sup>	Th BqKg <sup>-1</sup>	K BqKg <sup>-1</sup>	Absorbed dose rate nGyh <sup>-1</sup>		Observed dose rate nGyh <sup>-1</sup>	Annual effective equivalent dose μSvy <sup>-1</sup>	
							indoor	outdoor		indoor	outdoor
1	Sadras	12°31'60N	80°09'60E	9.06±0.3	11.14±1.4	542.08±24.6	61.81±4.2	34.12±3.5	75	303.20±8.2	41.84±2.1
2	Paandoor	12°58'60N	79°58'00E	9.86±0.4	32.79±2.3	584.52±25.3	89.56±5.1	49.77±4.4	110	439.34±9.6	61.04±2.6
3	Paalur	12°55'60N	79°40'00E	12.45±0.4	53.85±3.2	668.23±26.2	121.12±7.2	67.60±5.2	150	594.16±10.3	82.90±3.2
4	Maduranthagam	12°46'00N	79°31'60E	10.14±0.3	24.36±2.6	697.12±29.1	89.58±6.3	49.48±4.6	90	439.44±9.8	60.68±2.8
5	Chengalpattu	12°42'60N	80°01'00E	8.86±0.2	7.29±1.1	707.13±30.2	70.82±5.9	38.73±3.9	100	347.40±8.4	47.50±2.4
6	Valajabath	12°55'60N	79°22'60E	7.65±0.1	10.38±1.0	824.08±31.3	82.93±5.8	45.17±4.3	110	406.84±8.9	55.39±2.8
7	Kanchipuram	12°49'60N	79°43'00E	17.03±0.3	254.06±5.6	755.31±29.6	351.26±9.2	198.03±8.6	350	1723.12±14.6	242.86±4.8
8	Perumbakkam	12°50'00N	79°36'00E	10.05±0.2	21.76±2.1	873.6±28.4	100.96±6.6	55.41±5.2	120	495.26±7.3	67.96±3.2
9	Kaveripakkam	12°51'00N	79°30'00E	9.86±0.1	33.74±2.4	826.31±28.6	110.19±6.7	60.76±5.4	110	540.54±7.9	74.52±3.4
10	Pudhupadi	12°52'00N	79°24'60E	11.21±0.2	44.16±3.1	703.11±26.3	112.51±6.8	62.53±5.6	120	551.94±7.7	76.69±3.6
11	Walajapet	12°53'60N	79°21'60E	11.46±0.2	48.78±3.3	834.28±28.7	128.37±6.3	71.16±5.8	180	629.75±8.4	87.27±4.2
12	Ranipet	12°55'60N	79°19'60E	11.57±0.2	51.98±3.6	852.19±28.8	133.41±7.1	73.97±5.9	150	654.47±8.3	90.71±4.3
13	Vizharam	12°55'00N	79°15'60E	10.12±0.1	25.14±2.4	826.13±29.0	100.88±4.9	55.51±4.8	125	494.85±6.8	68.07±3.8
14	Rathnagiri	12°52'60N	79°12'60E	5.64±0.4	20.59±2.1	654.29±27.3	79.16±4.6	43.37±4.7	135	388.33±5.9	53.19±2.9
15	Sathuvancheri	12°53'60N	79°09'00E	7.06±0.3	42.46±2.8	692.36±27.2	107.19±6.4	59.24±5.2	105	525.81±7.8	72.65±3.2

Continued....

S.No.	Location	Latitude	Longitude	U BqKg <sup>-1</sup>	Th BqKg <sup>-1</sup>	K BqKg <sup>-1</sup>	Absorbed dose rate nGyh <sup>-1</sup>		Observed dose rate nGyh <sup>-1</sup>	Annual effective equivalent dose μSvy <sup>-1</sup>	
							indoor	outdoor		indoor	outdoor
16	Vellore	12°55'60N	79°07'00E	9.03±0.2	62.52±2.8	731.4±26.3	133.64±5.8	74.26±3.6	120	655.59±6.9	91.07±4.1
17	Melmanavur	12°55'00N	79°04'60E	8.52±0.1	46.52±2.3	698.42±26.2	113.05±5.7	62.65±3.4	130	554.59±5.9	76.84±3.6
18	Virungipuram	12°55'00N	79°01'00E	8.91±0.1	21.15±1.6	707.18±28.1	86.10±4.9	47.39±2.7	120	422.36±6.3	58.12±2.9
19	Kothikuppam	12°55'00N	78°57'60E	8.41±0.2	18.63±1.4	743.68±27.8	85.97±4.8	47.18±2.5	115	421.74±6.4	57.86±3.1
20	Pallikonda	12°55'60N	78°55'60E	8.67±0.2	6.13±1.2	756.28±27.3	73.40±4.3	40.04±2.3	140	360.09±4.8	49.11±2.8
21	Madhanoor	12°53'60N	78°52'60E	8.84±0.3	20.89±2.2	884.78±28.2	100.15±5.1	54.83±3.6	140	491.31±5.2	67.25±3.4
22	Melpatti	12°51'60N	78°57'00E	8.62±0.2	24.68±2.4	867.12±27.3	102.75±5.2	56.34±3.8	110	504.07±5.9	69.10±3.6
23	vadapudupatti	12°42'00N	78°48'60E	8.96±0.4	27.45±2.6	796.15±28.4	100.27±4.9	55.16±3.2	110	491.86±6.3	67.65±3.5
24	Ambur	12°46'00N	78°42'00E	9.03±0.4	33.78±3.1	731.16±26.3	102.01±5.4	56.34±3.9	180	500.41±7.1	69.10±3.8
25	Jothiveeraraghavapuram	12°44'60N	78°40'60E	8.75±0.3	19.95±2.5	779.8±26.8	90.56±6.2	49.70±2.7	140	444.25±6.3	60.95±2.9
26	Gollakuppam	12°42'00N	78°39'60E	8.58±0.2	24.15±2.3	840.63±27.2	100.00±5.8	54.86±3.6	125	490.57±6.8	67.28±3.6
27	Vaniambadi	12°40'00N	78°37'00E	8.93±0.3	22.79±2.6	821.96±27.8	97.21±4.8	53.36±3.9	140	476.88±6.7	65.44±3.4
28	Ambalur	12°38'00N	78°35'60E	18.44±0.4	52.42±3.1	483.49±24.3	108.31±6.3	61.32±4.2	140	531.34±6.9	75.20±4.1
29	Avarakuppam	12°39'60N	78°34'60E	9.62±0.2	19.66±1.8	532.67±25.2	70.77±3.9	39.26±3.8	110	347.15±5.8	48.15±2.8
30	Kanaganachiammankoil	12°37'60N	78°33'60E	8.83±0.2	11.64±1.6	858.22±30.3	87.82±4.2	47.93±4.1	120	430.81±7.2	58.78±3.3
Max				18.44±0.4	254.06±5.6	884.78±28.2	351.26±9.2	198.03±8.6	350	1723.12±14.6	242.86±4.8
Min				5.64±0.4	6.13±1.2	483.49±24.3	61.81±4.2	34.12±3.5	75	303.20±8.2	41.84±2.1
Mean				9.81±0.3	36.49±2.4	742.46±26.5	106.39±6.8	58.85±4.2	132.33	521.92±8.6	72.17±3.4

**Table 2:** The mean activity concentrations (BqKg<sup>-1</sup>) of <sup>238</sup>U, <sup>232</sup>Th and <sup>40</sup>K for different states of India

Sl.No.	Location	<sup>238</sup> U BqKg <sup>-1</sup>	<sup>232</sup> Th BqKg <sup>-1</sup>	<sup>40</sup> K BqKg <sup>-1</sup>	Reference
<b>Soil</b>					
1	Kalpakkam, T.N	5-71	15-776	200-854	Kannan et al. (2002) <sup>4</sup>
2	Bhuvaneswar, Orissa	18-30	33-80	213-247	Vijayan and Behera (1999) <sup>5</sup>
3	Coonoor(Ooaty), T.N.	BDL-49	4-224	14-731	Selvasekarapandian et al.(1999a) <sup>6</sup>
4	Gudalore, T.N.	17-62	19-272	78-596	Selvasekarapandian et al.(2000) <sup>8</sup>
5	Narora, U.P.	32-65	46-90	469-756	Verma et al. (1998) <sup>9</sup>
6	Rawatbhata, Rajasthan	17-40	27-67	127-49	Verma et al. (1998) <sup>9</sup>
7	Udagamandalam, (Ooty taluk), T.N.	0-88	26-226	96-444	Selvasekarapandian et al.(1999b) <sup>7</sup>
8	Ullal, Karnataka	546	2971	268	Radhakrishna et al. (1993) <sup>10</sup>
9	Uttarpradesh	12-25	20-25	538-1018	Mishra and Sadasivam(1971) <sup>11</sup>
<b>Beach Sand</b>					
10	Kalpakkam, T.N	36-258	352-3872	324-405	Kannan et al. (2002) <sup>4</sup>
11	Ullal, Karnataka	374	158	158	Radhakrishna et al. (1993) <sup>10</sup>
<b>River sediment</b>					
12	Cauvery river, T.N.	10.31	27.83	416.73	Murugesan et al.(2011) <sup>26</sup>
13	Bharadhapuzha,	41.86( <sup>226</sup> Ra)	54.86	477.75	Krishnamoorthy et. al.(2013) <sup>27</sup>
14	Palar River, T.N.	10.48	38.28	727.51	Present study

**Table 3:** The mean activity concentrations (BqKg<sup>-1</sup>) of <sup>238</sup>U, <sup>232</sup>Th, and <sup>40</sup>K for different countries in the world

Sl.No.	Country	<sup>238</sup> U BqKg <sup>-1</sup>	<sup>232</sup> Th BqKg <sup>-1</sup>	<sup>40</sup> K BqKg <sup>-1</sup>	Reference
1	China	62	90	524	Zigiang et al.(1998) <sup>28</sup>
2	USA	34	36	472	Delune et al. (1986) <sup>29</sup>
3	Republic of Ireland	37	26	350	Mc Aulay and Moran (1988) <sup>30</sup>
4	Greece	214	43	1130	Travidan et al. (1996) <sup>31</sup>
5	France	37	38	599	Lambrechts et al. (1992) <sup>32</sup>
6	Bangladesh	38	66	272	Mantazul et al. (1999) <sup>33</sup>
7	Taiwan	18	28	479	Chu et al. (1992) <sup>34</sup>
8	Egypt	17	18	316	Ibrahiem et al. (1993) <sup>35</sup>
9	Kuwait	36	6	227	Saad et al. (2002) <sup>36</sup>
10	Nigeria	16	24	35	Arogunjo et al. (2004) <sup>37</sup>
11	World	35	30	400	UNSCEAR (2000) <sup>1</sup>

### 3.3 Dose calculation

UNSCEAR [1] has given the dose conversion factors for converting <sup>238</sup>U, <sup>232</sup>Th and <sup>40</sup>K into doses (nGyh<sup>-1</sup> per Bqkg<sup>-1</sup>) as 0.427, 0.662 and 0.043 to calculate D<sub>OUT</sub> using the following equation by European Commission, 1999[13]

$$D_{OUT} = (0.427 C_U + 0.662 C_{Th} + 0.043 C_K) \text{ nGyh}^{-1}$$

and 0.92, 1.1 and 0.081 are used as conversion factor to calculate  $D_{IN}$

$$D_{IN} = (0.92 C_U + 1.1 C_{Th} + 0.081 C_K) \text{ nGyh}^{-1}$$

Where  $C_U$ ,  $C_{Th}$  and  $C_K$  are the activity concentrations ( $\text{Bqkg}^{-1}$ ) of uranium, thorium and potassium in sediments respectively. The mean indoor ( $106.39 \pm 6.8$ ) and outdoor ( $58.85 \pm 4.2$ ) absorbed dose rate  $\text{nGyh}^{-1}$  is higher than the world average. The contribution of the mean  $^{238}\text{U}$ ,  $^{232}\text{Th}$  and  $^{40}\text{K}$  activities in  $\text{nGyh}^{-1}$  to the mean absorbed dose rate is 7.1%, 41.04% and 54.26%.

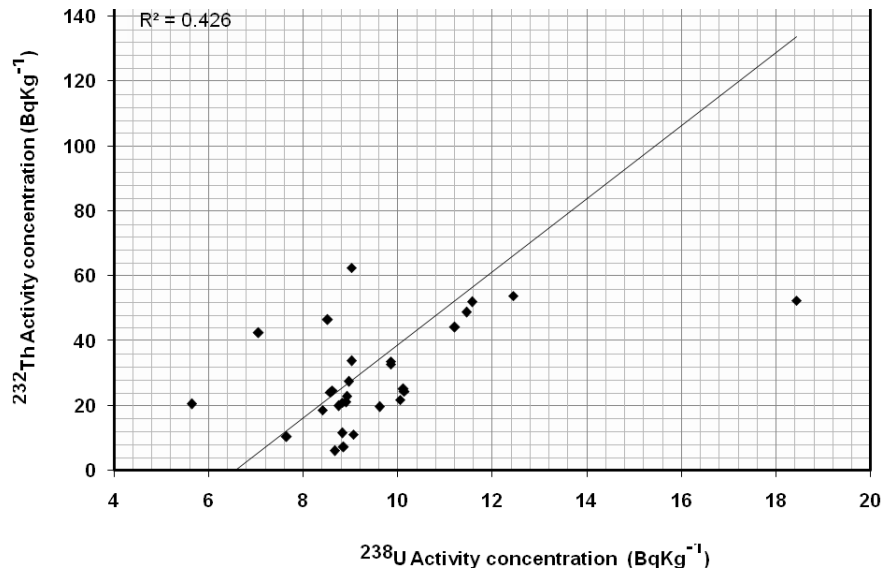


**Figure 3.** Correlation between  $^{238}\text{U}$  and  $^{232}\text{Th}$

In situ gamma dose rate at 1m above the ground has also been measured using the ERDM in each location of the river and the values are tabulated in Table 1. The observed dose rates are positively correlated with calculated absorbed dose rates with strong correlation coefficient ( $R = 0.90$ ) as shown in Fig.4. The ERDM dose rates (observed) are nearby two times higher than the absorbed dose rate values. This difference may be due to background contribution from cosmic rays.

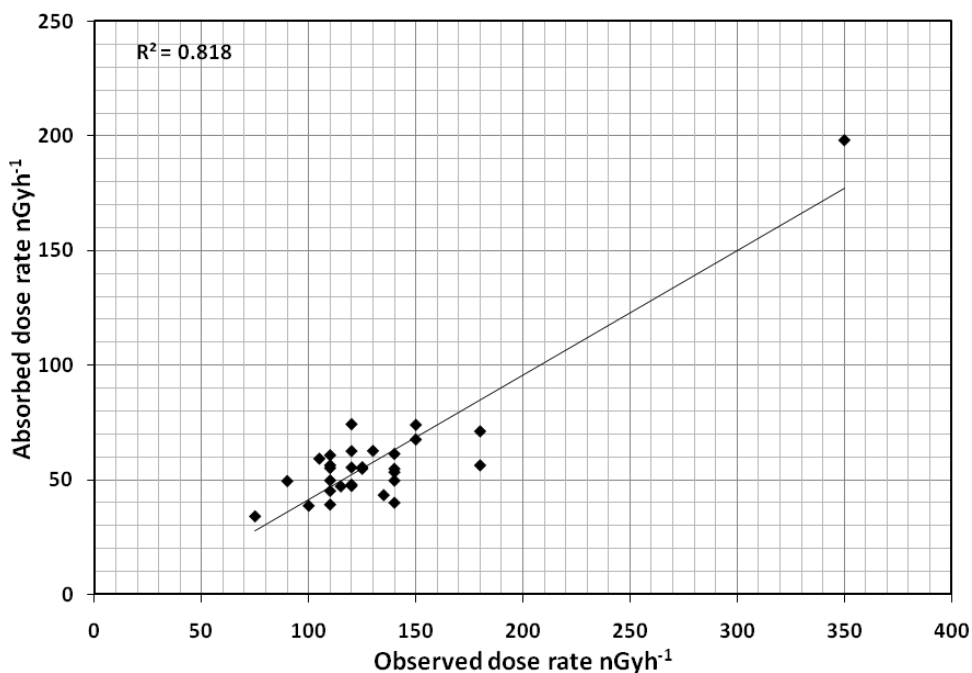


**Figure 4.** Correlation between absorbed dose rate and observed dose rate

A typical resident in a location, both male and female would spend about 8hrs of the day in an office (or) classroom or laboratory, 12 hrs indoors and the remaining 4hrs outdoors. This applies to the greater part of the population in a location who are either office workers or pupils/students. Hence 4/24 or 0.17 was adopted as the outdoor occupancy factor (20%) with the conversion factor of  $0.70\text{SvGy}^{-1}$  to convert absorbed dose rate in air ( $\text{nGyh}^{-1}$ ) to annual effective equivalent dose ( $\mu\text{Svy}^{-1}$ ) for this study (Ajayi, 2002). The indoor and outdoor annual effective equivalent dose varies between  $303.20\pm 8.2$ ,  $41.84\pm 2.1$   $\mu\text{Svy}^{-1}$  (site no.1) and  $1723.12\pm 14.6$ ,  $242.86\pm 4.8$   $\mu\text{Svy}^{-1}$  (site no.7) with a mean of  $521.92\pm 8.6$ ,  $72.17\pm 3.4$   $\mu\text{Svy}^{-1}$  respectively, those are higher than the world average  $70\mu\text{Svy}^{-1}$

### 3.4 Radioactive hazards

#### 3.4.1 Radium equivalent

Normally river sediments are used in building construction; so the radioactive nature of the materials is also very important. The total activity does not provide as an exact indication of the radiation hazard associated with the materials. A common index is defined in terms of radium equivalent activity ( $Ra_{eq}$ ) as given by the equation[14].

$$Ra_{eq} = C_U + A C_{Th} + B C_K$$

where  $C_U$ ,  $C_{Th}$  and  $C_K$  are the activity concentration of  $^{238}\text{U}$ ,  $^{232}\text{Th}$  and  $^{40}\text{K}$  ( $\text{Bqkg}^{-1}$ ) respectively and, A and B are constants. For the safe utilization of materials, the annual limit on the external gamma ray dose (1.5mSv), this corresponds to the value of  $370\text{Bqkg}^{-1}$  for radium equivalent.

From Table 4, it is observed that the site no. 7 shows the maximum of  $438.49\pm 9.2\text{Bqkg}^{-1}$  and the minimum of  $66.73\pm 5.6\text{Bqkg}^{-1}$ (site no. 1). For the estimation of radiological consequences instead of comparing the average values, maximum value is taken into account. The maximum  $Ra_{eq}$  is slightly higher than the world average ( $370 \text{Bqkg}^{-1}$ ). Rizzo et al. [15] reported the mean value of silicic sand is two times lower than the present study and ten times lower than the world average ( $370 \text{Bqkg}^{-1}$ ). In the present study the low concentration of  $Ra_{eq}$  value may be related to the transportation of radioactive materials by weathering, sedimentation and maximum water flow due to heavy rainfall in its origin.

#### 3.4.2 Correlation between $^{232}\text{Th}$ and $Ra_{eq}$

The linear correlation between  $Ra_{eq}$  and  $^{232}\text{Th}$  as shown in Fig.5 may indicate that the river mouth from laterite origin. Similar findings are reported soil samples of Karnataka [16,17]. The same state is the origin of Palar river.

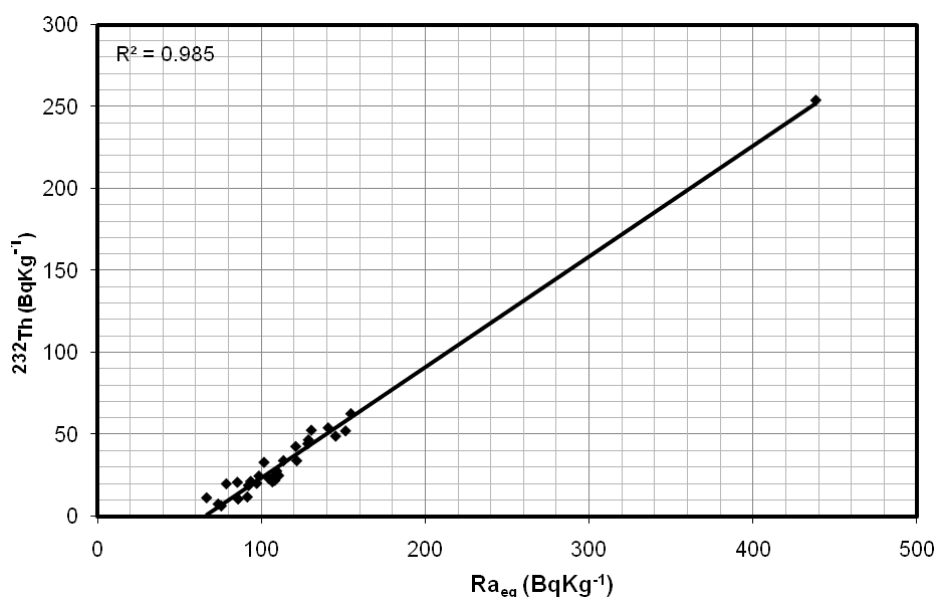


Figure 5. Correlation between  $Ra_{eq}$  and  $^{232}\text{Th}$



**Table 4:** Hazard indices, radium equivalent, radioactive heat production rate, magnetic susceptibility and weight of the magnetic minerals

Site No.	$H_{ex}$	$H_{in}$	$Ra_{eq}$ $BqKg^{-1}$	RHP $\mu Wm^{-3}$	ELCR		$\chi \times 10^{-8}$ $m^3 Kg^{-1}$	Weight of magnetic minerals in mg	Extinction Coefficient $cm^2/mg$		Quartz + Feldspar
					indoor	outdoor			Quartz	Feldspar	
					1	0.1802±0.02			0.2047±0.04	66.73±5.6	
2	0.2748±0.04	0.3014±0.06	101.76±6.3	0.5771±0.06	1.54±0.06	0.21±0.03	38.8	247	217.42	30.85	248.27
3	0.3805±0.06	0.4141±0.07	140.91±6.8	0.8770±0.09	2.08±0.09	0.29±0.03	28.4	320	391.76	61.86	453.62
4	0.2664±0.05	0.2938±0.03	98.65±5.8	0.5366±0.06	1.54±0.06	0.21±0.01	26.3	254	256.17	54.21	310.38
5	0.1991±0.03	0.2231±0.02	73.73±5.4	0.3389±0.04	1.22±0.03	0.17±0.01	28.4	187	162.22	32.59	194.81
6	0.2321±0.04	0.2528±0.05	85.95±5.7	0.3928±0.05	1.42±0.04	0.19±0.01	17.4	210	570.78	161.8	732.58
7	1.1840±0.31	1.2300±0.52	438.49±9.2	3.3128±0.45	6.03±0.2	0.85±0.04	279.7	620	301.34	30.81	332.15
8	0.2928±0.03	0.3200±0.06	108.43±4.3	0.5697±0.07	1.73±0.04	0.24±0.01	26.2	249	295.2	72.68	367.88
9	0.3287±0.07	0.3554±0.07	121.73±5.3	0.7050±0.09	1.89±0.07	0.26±0.01	61.8	250	234.67	82.63	317.30
10	0.3470±0.08	0.3773±0.05	128.50±5.4	0.7977±0.08	1.93±0.08	0.27±0.02	279.7	245	173.94	111.22	285.16
11	0.3928±0.05	0.4237±0.08	145.45±5.8	0.8878±0.07	2.20±0.07	0.31±0.02	55.2	328	168.23	76.54	244.77
12	0.4091±0.04	0.4404±0.07	151.52±5.7	0.9111±0.05	2.29±0.08	0.32±0.03	16.7	290	162.61	41.71	204.32
13	0.2962±0.06	0.3235±0.05	109.68±5.3	0.6265±0.07	1.73±0.05	0.24±0.01	9.1	280	210.66	61.082	271.74
14	0.2308±0.02	0.2460±0.01	85.46±4.9	0.4597±0.05	1.36±0.03	0.19±0.01	57.9	236	296.76	87.47	384.23
15	0.3270±0.04	0.3460±0.04	121.09±5.6	0.7269±0.08	1.84±0.09	0.25±0.02	52.1	340	252.31	56.78	309.09

Continued ....

Site No.	$H_{ex}$	$H_{in}$	$Ra_{eq}$	$BqKg^{-1}$	RHP $\mu Wm^{-3}$	ELCR X $10^{-3}$		$\chi \times 10^{-8}$ $m^3 Kg^{-1}$	Weight of magnetic minerals in mg	Extinction Coefficient $cm^2/mg$		Quartz + Feldspar
						indoor	outdoor			Quartz	Feldspar	
16	0.4179±0.08	0.4423±0.03	154.75±7.3	1.0391±0.21	2.29±0.09	0.32±0.04	44.6	380	187.38	49.53	236.91	
17	0.3478±0.06	0.3709±0.04	128.82±6.8	0.8110±0.07	1.94±0.08	0.27±0.02	51.3	320	171.34	49.65	220.99	
18	0.2528±0.04	0.2768±0.01	93.61±5.6	0.5568±0.04	1.48±0.04	0.20±0.07	52.6	267	168.43	50.21	218.64	
19	0.2493±0.04	0.2720±0.04	92.31±5.7	0.5129±0.06	1.48±0.06	0.20±0.04	33.69	281	246.71	61.34	308.05	
20	0.2043±0.05	0.2278±0.03	75.67±6.1	0.3566±0.04	1.26±0.04	0.17±0.02	22.6	267	279.51	66.3	345.81	
21	0.2885±0.07	0.3124±0.04	106.84±7.4	0.5438±0.06	1.72±0.09	0.24±0.04	31.3	320	459.12	132.05	591.17	
22	0.2989±0.08	0.3222±0.06	110.68±7.6	0.5923±0.07	1.76±0.05	0.24±0.08	33.7	296	446.15	125.63	571.78	
23	0.2957±0.09	0.3199±0.05	109.52±7.5	0.6257±0.08	1.72±0.03	0.24±0.04	37.1	289	411.27	86.27	497.54	
24	0.3068±0.06	0.3312±0.07	113.63±7.3	0.6785±0.05	1.75±0.07	0.24±0.01	39.8	273	373.19	76.41	449.60	
25	0.2628±0.07	0.2864±0.03	97.32±6.4	0.5565±0.03	1.55±0.06	0.21±0.06	27.6	268	306.21	69.61	375.82	
26	0.2912±0.08	0.3144±0.01	107.84±7.5	0.6038±0.04	1.72±0.05	0.24±0.09	25.3	295	251.63	67.12	318.75	
27	0.2830±0.09	0.3071±0.06	104.81±8.1	0.5676±0.05	1.67±0.07	0.23±0.05	24.5	245	177.11	65.82	242.93	
28	0.3527±0.06	0.4026±0.07	130.63±8.2	0.9877±0.06	1.86±0.10	0.26±0.02	136.7	362	88.39	22.26	110.65	
29	0.2126±0.04	0.2386±0.03	78.75±6.3	0.4753±0.08	1.22±0.03	0.17±0.03	20.12	278	481.77	117.83	599.60	
30	0.2472±0.05	0.2711±0.04	91.56±7.2	0.4944±0.09	1.51±0.05	0.21±0.08	19.31	229	365.16	117.61	482.77	
Max	1.1840±0.31	1.2300±0.52	438.49±9.2	3.3128±0.45	6.03±0.2	0.85±0.04	279.7	620	570.78	161.80	732.58	
Min	0.1802±0.02	0.2047±0.04	66.73±5.6	0.3389±0.04	1.06±0.02	0.15±0.02	9.1	210	88.39	22.26	110.65	
Mean	0.3200±0.06	0.3500±0.06	119.16±7.3	0.7200±0.08	1.83±0.7	0.25±0.04	53.12	288.7	281.22	72.09	353.30	

### 3.4.3 Hazard indices

The other quantities indicating the radiological hazards are external ( $H_{ex}$ ) and internal ( $H_{in}$ ) hazard indices and are defined by the following relations [13]:

$$H_{ex} = C_U/370 + C_{Th}/259 + C_K/4810 \leq 1$$

$$H_{in} = C_U/185 + C_{Th}/259 + C_K/4810 \leq 1$$

where  $C_U$ ,  $C_{Th}$  and  $C_K$  are the activity concentrations of U, Th and K in  $Bqkg^{-1}$ . The internal exposure to radon ( $^{222}Rn$ ) and its decay products is controlled by internal hazard index ( $H_{in}$ ) and for safe use, this index must be less than unity. From Table 4, the maximum values of  $H_{ex}$  and  $H_{in}$  are observed in site no. 7 ( $1.184 \pm 0.31$ ,  $1.230 \pm 0.52$ ). The hazard indices are higher than unity, which may cause harm to people living in this region.

### 3.4.4 Radioactive heat production (RHP) rate

During the last few decades, the assessment of the amount of radioactive elements, the major internal heat source of the earth, was the subject of several studies due to its importance in modeling the thermal evaluation of the lithosphere. The radioactive isotopes  $^{238}U$ ,  $^{232}Th$  and  $^{40}K$  contribute most of the terrestrial heat flow. These elements are fundamental for understanding the nature of the mantle, crust of the earth and their heat generating potential.

In the present study, an attempt has been made to find out the radioactive heat production rate at different sites using the relation given by Rybach [18].

$$A = 10^{-5} \rho (9.52 C_U + 2.56 C_{Th} + 3.48 C_K)$$

where A is radioactive heat production rate expressed in  $\mu Wm^{-3}$ ,  $\rho$  is the sample density in  $Kgm^{-3}$ ,  $C_U$  and  $C_{Th}$  are the uranium and thorium concentration in ppm and  $C_K$  is the total potassium concentration in %. In the present study, the heat production rate varies between  $0.3389 \pm 0.04 \mu Wm^{-3}$  (site no.5) and  $3.3128 \pm 0.45 \mu Wm^{-3}$  (site no.7) with a mean value of  $0.7200 \pm 0.08 \mu Wm^{-3}$ . In the present study the low RHP rate (below  $1 \mu Wm^{-3}$ ) except site no. 7 and 16. Here the overall heat generation mainly depends on  $^{232}Th$  amount and its contributions to RHP are 59.19%. However, an increase in the concentrations of  $^{238}U$ ,  $^{232}Th$  and  $^{40}K$  reflects the integrated effect of heat production rate.

### 3.4.5 Excess lifetime cancer risk (ELCR)

Excess life time cancer risk (ELCR) is calculated using the following equation and presented in Table 4.

$$ELCR \text{ Indoor} = AEDE \text{ Indoor} * DL * RF$$

$$ELCR \text{ Outdoor} = AEDE \text{ Outdoor} * DL * RF$$

where AEDE, DL and RF is the annual effective dose equivalent, duration of life (70years) and risk factor ( $Sv^{-1}$ ), fatal cancer risk per sievert. For stochastic effects, ICRP60 uses values of 0.05 for the public[19]. The (ELCR) for outdoor exposure is ranged from  $0.15 \pm 0.02$  to  $0.85 \pm 0.04$  with an average value of  $0.25 \pm 0.04$ , which is lower than world average of 0.29. For indoor exposure it is from  $1.06 \pm 0.02$  to  $6.03 \pm 0.2$  with an average of  $1.83 \pm 0.7$ , which is 1.58 times greater than the indoor world average (UNSCEAR, 2000)<sup>1</sup>. The (ELCR) for outdoor exposure is ranged from  $0.15 \pm 0.02$  to  $0.85 \pm 0.04$  with an average value of  $0.25 \pm 0.04$ , which is lower than world average of 0.29. For indoor exposure it is from  $1.06 \pm 0.02$  to  $6.03 \pm 0.2$  with an average of  $1.83 \pm 0.7$ , which is 1.58 times greater than the indoor world average (1.16). But site no. 7 shows indoor ELCR as 5.2 times greater than the world average. Numerous cancer deaths are annually reported in and around the site as per government medical record.

### 3.6 Distribution of quartz and feldspar

FTIR spectra are recorded for all the sampling sites and Comparing the observed frequencies with available literature [20-22], the minerals such as quartz, feldspar, kaolinite in different composition, nacrite, montmorillonite, illite, chlorite, gibbsite, carbonates, sepiolite and magnesium oxalate are identified. The observed IR absorption frequencies and its corresponding minerals are tabulated in Table 5.

The relative distribution of quartz and feldspar among the various sites of the present study [23,24] are determined using extinction coefficient of the characteristic peaks at  $778cm^{-1}$  and  $640cm^{-1}$  respectively which are shown in Table 4 and these values are correlated with radioactivity measurements. Rizzo et. al.[15] suggest that Si is good safety index to select the materials of low radiological impact in geological areas of prevalent magmatic origin. But in the present study, the distribution of quartz, feldspar gives no obvious trend with individual activities ( $^{238}U$ ,  $^{232}Th$  and  $^{40}K$ ) and absorbed dose rate. This suggests Si is not an index to select low radiological area.

**Table 5:** Observed absorption frequencies ( $\text{Cm}^{-1}$ ) from FTIR spectra of the samples [23]

Sl.No	Mineral Name	Observed Frequency $\text{cm}^{-1}$	Site Number
1	Chlorite	440	1,14 & 15
2	Sepiolite	450	16, 23
3	Quartz	458-462	1-30
4	Sepiolite	470	16, 23
5	Orthoclase	530-535	1-30
6	Microcline	580-585	1-30
7	Orthoclase	629-650	1-30
8	Gibbsite	665-675	2,4,6,7,2,8-21,24,27 & 28
9	Quartz	690-694	1-30
10	Albite	729-732	1-30
11	Quartz	777	1-30
12	Montmorillonte	890-895	18,19, 21,26,30
13	Kaolinite	912-915	9,18,19,22,25 & 29
14	Kaolinite	1004-1006	9,18,19,22,25 & 29
15	Kaolinite	1030-1032	9,18,19,22,25 & 29
16	Albite	1038-1045	1-8,10-17, 20, 21,26 & 28
17	Quartz	1080-1083	1-18, 20 21,23,24&27
18	Kaolinite	1100-1110	9,18,19,22,25 & 29
19	Albite	1135-1150	1-30
20	Magnesium Oxalate	1375-1377	9,18,19 & 23
21	Cerrussite	1384-1388	11,18,26 & 28
22	Calcite	1400-1440	9,11,13,18-21, 24 & 27
23	Gibbsite	3527	2,4,6,7,12,18-21,24,27 &28
24	Kaolinite	3620,3654 & 3697	1-30

### 3.7 Magnetic susceptibility

According to Nagamalleswara Rao [25], the magnetite is responsible for magnetic susceptibility and the monazite is responsible for radioactivity. When compare magnetic susceptibility with absorbed dose rate of the sediment samples, some of the following results arrived.

1. High radiation level and low magnetic susceptibility may indicate the sediments with low magnetite and high concentration of monazite as in the site no.12.(with reference to ref.25)
2. Low radiation level and high magnetic susceptibility may indicate the sediments with abundant magnetite and low/negligible monozite content as in the site no.14.(with reference to ref.25)
3. Intermediate levels of radiation and magnetic susceptibility may indicate the sediments with equal abundance of magnetite and monazite as in the site no.10. (with reference to ref.25)
4. High magnetic susceptibility and high radioactivity may indicate the abundant magnetite and monazite as in the site no.7. (with reference to ref.25)

From the above observations, the correlation between magnetic susceptibility and absorbed dose rate ( $R=0.68$ ) is found to be weak as shown in Fig. 6, because the resultant magnetic susceptibility is obtained from the resultant effect of dia, para, ferri, and antiferro magnetic materials. Quartz is most popular diamagnetic material. It has very minimum and negative susceptibility values. In the present study, quartz is dominant mineral. So the resultant susceptibility may be slightly varied by different magnetic properties of the sediments like diamagnetism. But the weight of the magnetic minerals gives good correlation with absorbed dose rate ( $R=0.91$ ) as shown in Fig. 7. To confirm this result, the site no.7 has been selected and the activity concentration values are measured after separating the magnetic mineral content using electromagnet. This result shows that the activity concentration and absorbed dose rate of the respective sample is decreased i.e., these values are very low when compared to before separation and world average. It is observed that weight of the magnetic minerals is an index to select the sediments of low or high radiological impact of Palar River.

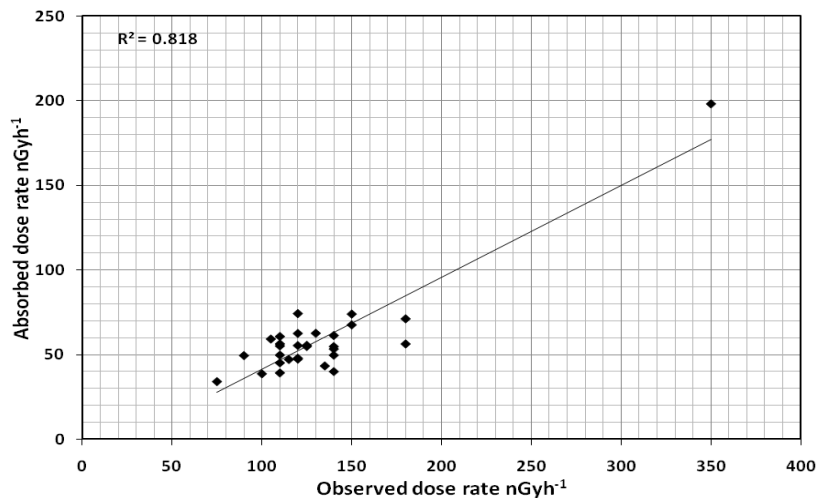


**Figure 6.** Correlation between absorbed dose rate and magnetic susceptibility

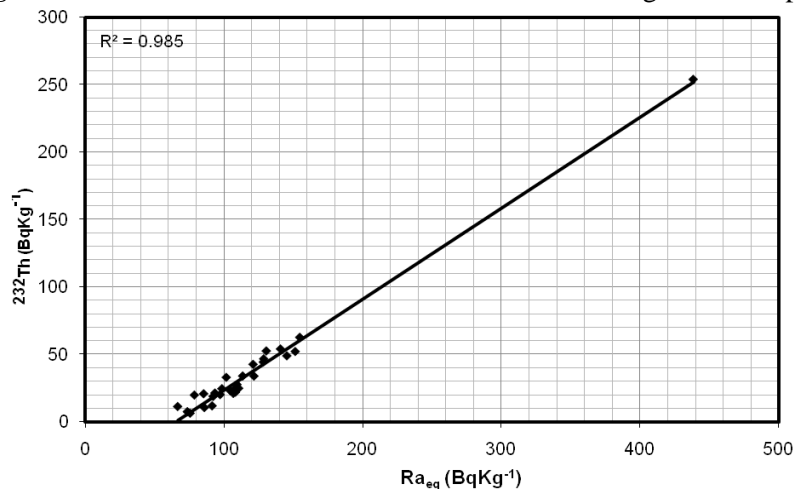


**Figure 7.** Correlation between Absorbed dose rate and weight of the magnetic minerals

## Conclusion

It is clear from the data of the gamma ray spectroscopic analysis in the present study of sediment samples that the levels of mean activity concentration of  $^{238}\text{U}$ ,  $^{232}\text{Th}$  and  $^{40}\text{K}$  is lower than the world average. The mean absorbed dose rate is also lower than the world average. The mean annual effective equivalent dose is 1.03 times with that of world average ( $70\mu\text{Svy}^{-1}$ ). The mean value of  $R_{\text{eq}}$ ,  $H_{\text{ex}}$  and  $H_{\text{in}}$  found in the present study are lesser than the world average of  $370\text{Bqkg}^{-1}$ , 1 and 1 respectively. Therefore these sediments do not pose source of radiation hazard when used as building materials. Among all the sites, the site no. 3,7,9 to 12, 15, 16, 17 and 28 show the highest values of absorbed, observed, annual effective equivalent dose, radium equivalent hazard indices, RHP and indoor and outdoor ELCR. This implies that inhabitation of those areas are subjected to increased radiation exposure. So these sites are harmful to human health. Though the magnetic susceptibility cannot give any correlation with absorbed dose rate the weight of the magnetic minerals give positive correlation with absorbed dose rate,  $R_{\text{eq}}$  and RHP. Thus, the weight of the magnetic minerals is also an index to select low radiological impact of the sediments. The river sediments when used as a building material do pose a radiological threat within the dwellings. Locals should avoid the liberal use of the river sediments for construction purpose. Especially the site no. 7 shows very serious radiological effect. The people living in and around this area may be instructed to avoid using palur river sediment as building material. As per Health department, government of Tamilnadu records, numerous cancer deaths are annually reported.

## References

1. UNSCEAR (United Nations Scientific Committee on the effects of Atomic Radiation) 2000 United Nations New York, 2000.
2. Jamal Al-Jundi, *Radiat. Measur.* 35 (1971) 23-28.

3. UNSCEAR (United Nations Scientific Committee on the effects of Atomic Radiation) United Nations New York, 1988.
4. Kannan V., Rajan M.P., Iyengar M.A.R., Ramesh R., *Appl. Radiat. Isoto.* 57 (2002) 109.
5. Vijayan V., Behera S.N., Study of natural Radioactivity in soils of Bhubaneswar Proceedings of the Eight National Symposium on Environment Indira Gandhi Centre for Atomic Research Kalpakkam India, 146-147, 1999.
6. Selvasekarapandian S., Muguntha Manikandan N., Sivakumar R., Balasubramanian S., Venkatesan T., Meenakshi Sundaram V., Raghunath V.M., Gajendran V., *Radiat. Protec. Dosimet.* 82 (1999) 225-228.
7. Selvasekarapandian S., Sivakumar R., Muguntha manikandan N., Meenakshisundaram V., Raghunath V.M., Gajendran V., Measurements of natural radioactivity levels in soil in Coonoor Proceedings of the Eighth National Symposium on Environment Indira Gandhi Centre for Atomic Research Kalpakkam India, 160-163, 1999.
8. Selvasekara Pandian S., Sivakumar R., Manikandan N.M., MeenakshiSundaram V., Raghunath V.M., Gajendran V., *Appl. Radiat. Isot.* 52 (2000) 299-306.
9. Verma P.C., Gurg R.P., Sundaram M., Sharma L.N., Natural radioactivity in Rawatbhata and Narora soils Proceedings of the Seventh National Symposium on Environment Indian School of Mines Dhanbad-826004 India, 132-134, 1998.
10. Radhakrishna A.P., Somashekarappa H.M., Narayana Y., Siddappa K.A., *Heal. Phys.* 65 (1993) 390-395.
11. Mishra, V.C., Sadasivan, S., *J. Sci. Ind. Res.* 30 (1971) 59-62.
12. Abdelhady E.E., El Sayed A.M.A., Ahmed A.A., Hussein A.Z., *Radiat. Phy. Chem.* 44(1/2) (1994) 223-224.
13. U C (European Commission). (1999). Radiological protection principles concerning the natural radioactivity of building materials. In EC radiation protection, 112. Directorate General Environment, Nuclear Safety and Civil Protection.
14. Beretka J., Mathew P.J., *Heal. Phys.* 48 (1985) 87-95.
15. Rizzo S., Brai M., Basile S., Bellia S., Hauser S., *Appl. Radiat. Isoto.* 55 (2001) 259-265.
16. Narayana Y., Somashekarappa H.M., Karunakara N., Avadhani D.N., Mahesh H.M., Siddappa K., *Heal. Phys.* 80 (2001) 25-33
17. Yu-Ming L., Pei-Huo L., Ching-Jiang C., Ching-Chung H., *Heal. Phys.* 52 (1987) 805-811
18. Rybach L. Determination of heat production rate. Handbook of Terrestrial heat flow density Determinations Kluwer Dordredut. In Haenel R Rybach L Stegena L (Eds), 125-142.
19. Taskin H., Karavus M., Ay P., Topuzoglu A., Hindiroglu S., Karahan G., *J. Environ. Radio.* 100 (2009) 49.
20. Madejova J., *Vibrat. Spectros.* 31 (2003) 1-10.
21. Russell J.D., Infrared methods - A Hand Book of determinative methods in clay mineralogy, Ed. by Wilson MJ, Blackie and Son Ltd., New York, 133-173 (1987).
22. Ramasamy V., Murugesan S., Mullainathan S., *Bull. Pure and Appl. Sci.* 23F (2004) 1-2.
23. Ramasamy V., Mullainathan S., Murugesan S., *J. Curr. Sci.* 5(2) (2004) 599-606.
24. Ramasamy V., Dheenathayalu M., Ponnusamy V., Murgesan S., Mullainathan S., *J. Curr. Sci.* 3 (2003) 181
25. Nagamalleswara Rao B., *J. Geolo. Soc. India* 43 (1995) 669-675.
26. Murugesan S., Mullainathan S., Ramasamy V., Meenakshisundaram V., *Inter. J. Radia. Res.* 8 (2011) 211.
27. Krishnamoorthy N., Mullainathan S., Mehra R., Marcos Chaparro A.E., Mauro Chaparro A.E., *Radiat. Prot. Dosimet.* (2013) doi: 10.1093/rpd/nct288).
28. Ziquiang P., Yin Y., Mingqiang G., *Radiat. Protec. Dosimet.* 24 1988 29-38.
29. Delune R.D., Jones G.L., Smith C.J., *Heal. Phys.* 51 (1986) 239-244.
30. McAulay I.R., Moran D., *Radiat. Protec. Dosimet.* 224 (1988) 47-49.
31. Travidon G., Flouro H., Angelopoulos A., Sakellioou L., *Radiat. Protec. Dosimet.* 63 (1996) 63-67.
32. Lambrechts A., Foulquier L., Garnier-Laplace J., *Radiat. Protec. Dosimet.* 45 (1992) 253-256.
33. Mantazul I.C., Alam M.N., Hazari S.K.S., *Appl. Radiat. Isoto.* 51 (1999) 747-755.
34. Chu T.C., Weng P.S., Lin Y.M. *Radiat. Protec. Dosimet.* 45 (1992) 281-283.
35. Ibrahim N.M., Abd E.I., Ghani A.H., Shawky S.M., Ashraf E.M., Farouk M.A., *Heal. Phys.* 64 (1993) 297
36. Saad H.R., Al-Azmi D., *Appl. Radiat. Isoto.* 56 (2002) 991-997.
37. Arogunjo A.M., Farai I.P., Fuwape I.A., *Radiat. Protec. Dosimet.* 108 (2004) 73-77.